SETSCI conference proceedings
SETSCI Conference Proceedings
5 (2), 76-83, 2022

6th International Symposium on Innovative Approaches in Smart Technologies
December 8-10, 2022, Turkey

ISAS WINTER-2022

https://doi.org/10.36287/setsci.5.2.017

Development of a Torque Vectoring Strategy to improve Performance in Electric Vehicles with Individually Driven Wheels

Hamza Shabbir[1], Omer Cihan Kivanc[2]

[1*]Automotive Mechatronics and Intelligent Vehicles, Okan University, Istanbul, Turkey
[2]Electrical and Electronics Engineering, Okan University, Istanbul, Turkey
[*](hamshabbir@stu.okan.edu.tr)

Abstract – In this work, a new torque vectoring strategy is developed and the results are compared with those of existing controllers that are widely used for such applications in the existing literature. The objective of said strategy is to generate the corrective yaw moment through a differential of forces applied to the individual wheels of a vehicle in order to stabilize the vehicle and improve the overall performance in mixed conditions. A novel algorithm that combines different low-level controllers is constructed in order to best leverage the desired behaviors of each controller in different traction scenarios is presented. Both the existing controllers and the new strategy were compared by simulating a double lane change maneuver on a planar vehicle model at different traction levels in order to demonstrate the functionality and stability of the proposed approach. The results of these maneuvers are also used to understand the impact of the proposed torque vectoring strategy and existing controllers on the vehicle behavior.

Keywords –torque vectoring, SMC, planar vehicle, lateral stability, yaw control, vehicle stability

I. INTRODUCTION

Due to the recent advancements in electric vehicle technology, the overall performance of electric vehicles (EV) has markedly improved and with it brings a host of opportunities for development of performance and safety enhancing systems.

Vehicle dynamic stability is a key factor to consider when it comes to performance and the safety of the driver. Manufactures have been constantly developing and implementing new techniques to improve vehicle manoeuvrability and safety as for light vehicles, yaw dynamic stability is a critical point to control [1].

As the maximum tire forces that can be generated are limited, during extreme manoeuvers, these tire forces may saturate and cause the vehicle to deviate from its course, in addition to this, the steering response will also change reducing the chances of recovery. To counter this, systems like anti-lock braking system (ABS) and traction control (TC) are designed to alter the longitudinal response in such conditions. Whereas, the lateral response is dealt with by direct yaw moment control (DYC) methods such as the widely used electronic stability control (ESC).

ESC generates a yaw moment about the vehicle's vertical axis by braking specific tires in order to correct the yaw motion of the vehicle. From a safety point of view, it is an important addition to modern vehicles as it operates in safety critical situations. However, due to the fact that these systems rely on braking the individual wheels, the longitudinal performance of the vehicle is compromised. This will restrict the driver from exploiting the capabilities of the vehicle in situations where performance is a priority and has also been reported as being disruptive because of unexpected drops in speed [2].

Unlike ESC, torque vectoring (TV) relies on distributing the driving forces between the wheels thus the adverse effect on the longitudinal performance is minimized. TV can also prolong the drivability in conditions where the tire slip is increasing by managing the torque between the wheels before emergency systems like ESC and TC are finally deployed [3].

Managing these longitudinal forces in such a manner results in the utilisation of tires in respect of the cornering or the lateral forces which are important in achieving a faster lap-time or when an overall vehicle performance improvement is necessary.

Electric Torque Vectoring can be applied on vehicles which are driven by two or more electric motors. Independently driven wheels enable the TV system to operate as a passive or an active system, opening possibilities for different driving modes prioritising energy efficiency or performance.

Several different control strategies have been developed to implement TV like an integrated controller to prevent understeer [4], a gain-scheduled PID controller in [5], a super-twisting SMC in [6], and the use of LQR is discussed by many authors including [7], [8], and [9].

The above mentioned controllers are used exclusively or in a combination to determine the corrective yaw rate or any other parameter however the low-level distribution of torques is mostly only limited to one strategy for each vehicle which is meant to work in all conditions.

This paper proposes a low-level controller which switches between different torque distribution strategies driven by logic to maximize the operating region of a vehicle and improve the overall stability and handling in mixed driving conditions. A high-level controller generates the required corrective yaw moment which is then translated to torques at individual wheels through the low-level controller. The discussed control

architecture is then compared to existing torque distribution strategies.

II. VEHICLE MODEL

The vehicle models used in this study to design and evaluate the controller are the non-linear planar model and the linear bicycle model.

A. Linear Model

A standard bicycle model as shown in Fig. 1 is used to calculate the desired response which in our case is the desired yaw rate. By assuming that the motion is restricted to a plane and that the forces generated by the tires are operating in the linear region, the steady-state yaw rate response can be derived.

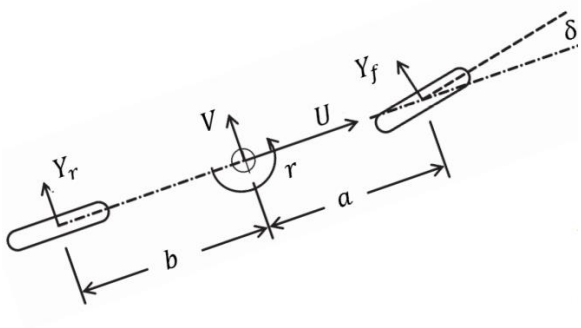

Fig. 1 Bicycle Model

The understeer gradient is:

$$K_{us} = \frac{m(bC_r - aC_f)}{(a+b)C_fC_r} \quad (1)$$

And the steering response can be expressed as:

$$r_{des} = \frac{U}{(a+b)(1+K_{us}U^2)}\delta \quad (2)$$

Combining equations (1) and (2) the desired yaw rate, r_{des} with respect to the steering angle and the longitudinal velocity will be as shown below.

$$r_{des} = \frac{U}{(a+b)(\frac{mU^2(aC_{alphaf} - bC_{alphar})}{2C_{alphaf}C_{alphar}(a+b)})}\delta \quad (3)$$

where; δ is the steering angle, C_{alpha} is the lateral tire stiffness coefficient, C_{sigma} is the longitudinal tire stiffness coefficient, a is the distance from the centre of gravity to the front axle, b is the distance from the centre of gravity to the rear axle, m is the vehicle mass, and U is the vehicle velocity.

The longitudinal velocity is taken as a user defined value throughout the simulations instead of the current vehicle speed.

In practical applications the desired yaw rate will be limited by a function of the tire-road friction coefficient:

$$r_{max} = \frac{\mu g}{U} \quad (4)$$

Here μ is the friction coefficient. However for comparison purposes, this limit will vary for different controllers due to its dependence on the current vehicle longitudinal velocity.

B. Planar Vehicle

The 3DOF double-track planar model, shown below in Fig. 2, is used to test the controller.

Only the longitudinal, lateral, and yaw dynamics are considered while the roll, pitch and bob motions are ignored. The mass of the vehicle is assumed to be at the centre of its gravity.

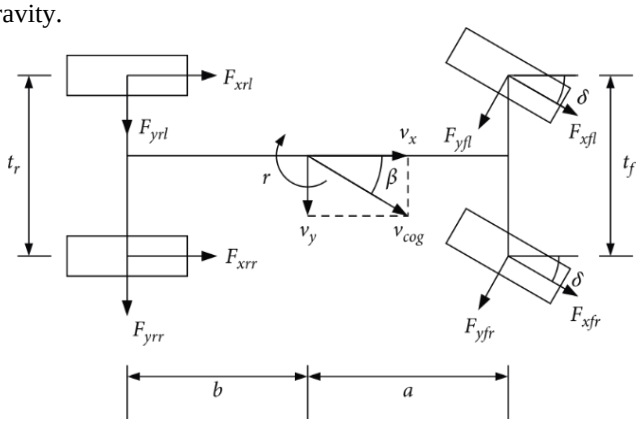

Fig. 2 Planar Vehicle Model

The equations corresponding to the planar vehicle model are as follows:

Longitudinal motion:

$$m(a_x - v_y r) = F_{xfl}\cos(\delta_f) - F_{yfl}\sin(\delta_f) + F_{xfr}\cos(\delta_f) - F_{yfr}\sin(\delta_f) + F_{xrr} + F_{xrl} \quad (3)$$

Lateral motion:

$$m(a_y - v_x r) = F_{xfl}\,sin(\delta_f) + F_{yfl}\,cos(\delta_f) + F_{xfr}\,sin(\delta_f) + F_{yfr}\,cos(\delta_f) + F_{yrr} + F_{yrl} \quad (5)$$

Yaw motion:

$$\dot{r}I_z = a(F_{xfl}\,sin(\delta_f) + F_{xfr}\,sin(\delta_f) + F_{yfl}\,cos(\delta_f) + F_{yfr}\,cos(\delta_f)) + \frac{t_f}{2}(F_{xfl}\cos(\delta_f) - F_{xfr}\cos(\delta_f) + F_{yfr}\,sin(\delta_f) - F_{yfl}\,sin(\delta_f)) + \frac{t_r}{2}(F_{xrl} - F_{xrr}) \quad (6)$$

where $t_{f,r}$ is the track width, F_{xij} and F_{yij} are the force components in the longitudinal and lateral direction respectively. The subscript 'ij' defines the tire such as FR, FL, RR, and RL.

C. Weight Transfer

The varying vertical load on the tires determine the amount of available forces each tire can produce. Static load and load transfer due to longitudinal and lateral forces are considered. The vehicle roll motion and suspension geometry are neglected.

Static load transfer is simply the overall mass distributed according to the relative position of the front and rear axles with respect to the centre of gravity as shown by the following equations:

$$F_{z,front} = \frac{mga}{a+b} \quad (7)$$

$$F_{z,rear} = \frac{mgb}{a+b} \quad (8)$$

As suspension geometry and roll motion of the vehicle are neglected, the lateral weight transfer is purely due to the lateral acceleration:

$$F_{z,lateral} = \frac{mha_y}{t_{f,r}} \quad (9)$$

where h is the height of the centre of gravity.

Similarly, the longitudinal load transfer can be written as:

$$F_{z,longitudinal} = \frac{mha_x}{a+b} \quad (10)$$

Combining the above equations:

$$F_{z,fl} = \frac{1}{2}F_{z,front} - \frac{1}{2}F_{z,longitudinal} + \frac{1}{2}F_{z,lateral} \quad (11)$$

$$F_{z,fr} = \frac{1}{2}F_{z,front} - \frac{1}{2}F_{z,longitudinal} - \frac{1}{2}F_{z,lateral} \quad (12)$$

$$F_{z,rl} = \frac{1}{2}F_{z,front} + \frac{1}{2}F_{z,longitudinal} + \frac{1}{2}F_{z,lateral} \quad (13)$$

$$F_{z,rr} = \frac{1}{2}F_{z,front} + \frac{1}{2}F_{z,longitudinal} - \frac{1}{2}F_{z,lateral} \quad (14)$$

Equations (11)-(14) represent the normal forces acting on each tire due to the weight transfer.

III. Tire Model

A. Wheel Dynamics

Fig. 3 below shows a simplified model of a single wheel where T denotes the torque applied by the motor, R_{eff} is the effective radius, ω is the angular velocity of the wheel, and F_x is the longitudinal force.

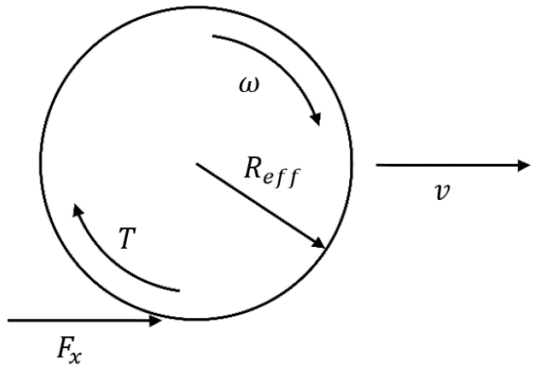

Fig. 3 Wheel Dynamics

The angular acceleration can be calculated using the torque acting on the tire:

$$\dot{\omega}_w = \frac{T_{wheel} - R_{eff}F_x}{I_w} \quad (15)$$

where I_w is the moment of inertia of the tire.

Due to the forces acting on the tire, the surface of the tire will deform and this will cause the surface to slip. This tire slip ratio, σ_x can be calculated as:

During acceleration:

$$\sigma_x = \frac{R_{eff}\omega_w - v}{R_{eff}\omega_w} \quad (16)$$

During deceleration:

$$\sigma_x = \frac{R_{eff}\omega_w - v}{v} \quad (17)$$

This slip ratio is later used for the calculation of forces in the selected tire model.

B. Dugoff Tire Model

The tire model used in this study is the Dugoff Tire Model. It approximates the tire forces in the linear and the non-linear region. These forces can be expressed using the following equations:

Longitudinal tire force:

$$F_x = C_\sigma \frac{\sigma_x}{1+\sigma_x} f(\lambda) \quad (18)$$

Lateral tire force:

$$F_y = C_\alpha \frac{\tan(\alpha)}{1+\sigma_x} f(\lambda) \quad (19)$$

$$f(\lambda) = \begin{cases} (2-\lambda)\lambda, & \lambda < 1 \\ 1, & \lambda \geq 1 \end{cases} \quad (20)$$

λ is a function of friction coefficient, μ, the normal force acting on the tire, the slip ratio, longitudinal and lateral stiffness coefficients and the side slip angle of the tire, α.

$$\lambda = \frac{\mu F_z(1+\sigma_x)}{2\{(C_\sigma\sigma_x)^2 + (C_\alpha \tan(\alpha))^2\}^{0.5}} \quad (21)$$

Consequently, tire slip values of each tire can be calculated using the following set of equations:

$$\alpha_{fr} = -\tan^{-1}\left(\frac{V+ar}{U+\frac{tf}{2}r}\right) + \delta \quad (22)$$

$$\alpha_{fl} = -\tan^{-1}\left(\frac{V+ar}{U-\frac{tf}{2}r}\right) - \delta \quad (23)$$

$$\alpha_{rr} = -\tan^{-1}\left(\frac{V-br}{U+\frac{tr}{2}r}\right) \quad (24)$$

$$\alpha_{rl} = -\tan^{-1}\left(\frac{V-br}{U-\frac{tr}{2}r}\right) \quad (25)$$

IV. Control Strategy

A. Torque Vectoring Principle

For a vehicle turning left, the weight transfer is towards the right of the vehicle thus the normal forces are higher for the right tires. Considering equal driving forces on a single axle as shown in Fig. 4 (a), the outer tire produces the same magnitude of longitudinal force as the inner tire which is the limiting factor here since its equal to the frictional force $F_{m,in}$ thus only the outer wheel is able to produce the maximum lateral force.

For a vehicle with TV, a longitudinal force difference, F_{delta}, is generated by reducing the torque from the inner wheel and adding the same magnitude of driving torque to the outer wheel. This causes an additional yaw moment to act on the axle.

With TV, as shown is Fig. 4 (b) the inner tire is able to produce a lateral force $F_{y,in}$ since $F_{x,in}$ is no longer equal to $F_{m,in}$. Such uneven distribution of the driving forces result in a yaw moment which reduces the steering effort as it assists in the turning of the vehicle. At the same time, the increase in the outer wheel longitudinal force $F_{x,out}$, causes $F_{y,out}$ to decrease but this is offset by the net increase in the lateral force across the axle.

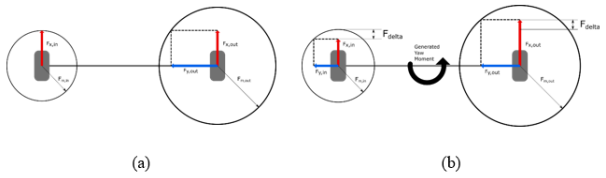

Fig. 4 (a) Without Torque Vectoring and (b) With Torque Vectoring

Through left-right TV, both wheels are now able to work within their limit and make use of the extra grip previously unutilised without sacrificing any longitudinal performance.

F_m is the product of the coefficient of friction and the normal force, F_z, acting on the tire.

$$F_m = \mu F_z \tag{26}$$

The maximum cornering force for each tire, $F_{y,max,i}$ where $i = 1,2,3,4$ represents the wheel, can be calculated using simple geometry:

$$F_{y,max,i} = \sqrt{({F_{m,i}}^2 - {F_{x,i}}^2)} \tag{27}$$

B. Control Laws

1) High Level Controller

A sliding mode controller is designed and used for comparison purposes. The approach is similar to the one discussed in [10] with changes, only the Yaw Rate is tracked in these simulations for the sake of clarity fair comparison of performances of different low level controllers.

The sliding surface is chosen to be:

$$s = r - r_{reference} \tag{28}$$

Differentiating the sliding surface:

$$\dot{s} = \dot{r} - \dot{r}_{reference} \tag{29}$$

$\dot{r}$ can be obtained by rewriting the yaw motion equation of the planar vehicle model and substituting $F_{xr,rl} = \rho F_{xf,rl}$:

$$\dot{r} I_z = a(F_{yfl}\cos(\delta_f) + F_{yfr}\cos(\delta_f)) - b(F_{yrl} - F_{yrr}) + \frac{t_f}{2}(F_{xfl}\cos(\delta_f) - F_{xfr}\cos(\delta_f)) + \rho\frac{t_r}{2}(F_{xfl} - F_{xfr}) \tag{30}$$

Here ρ can be used to set the degree of rear axle's contribution to the moment calculation.

Due to the differential driving forces, the yaw torque is denoted as:

$$M_{des} = \frac{t_r}{2}(F_{xfr} - F_{xfl}) \tag{31}$$

Setting $\dot{s} = -\eta s$, the desired corrective moment will be:

$$M_{des} = \frac{I_z}{\rho+\cos(\delta)}\left(-\frac{a}{I_z}\left(F_{yfl} + F_{yfr}\right)\cos(\delta) + \frac{b}{I_z}\left(F_{yrl} + F_{yrr}\right) - \eta s + \dot{r}_{des}\right) \tag{32}$$

In order to maintain a valid comparison, all parameters for the high level controller are fixed.

2) Low Level Controllers

Basic TV Low Level Controller:

A controller where the corrective torques are added to the base torque demanded by the driver. It is used by several authors like [8], [11], [12], [13] and [9]. This method is mostly used for RWD vehicles.

$$\Delta T = \frac{R_{eff} M_z}{2(\frac{d}{2})} \tag{33}$$

Since only one axle is active, the driver demand is divided equally so the resulting torques at the tires can be written as:

$$T_r = \frac{1}{2}T_{driver} + \Delta T \tag{34}$$

$$T_l = \frac{1}{2}T_{driver} - \Delta T \tag{35}$$

where d is the halftrack, R_{eff} is the effective radius of the tires and M_z is the corrective Yaw Moment generated by the high level controller.

Rear Wheel Drive + Front Torque Vectoring:

As the name suggests, here the rear wheels are solely driven by the torque from the driver and the front wheel forces are manipulated by the controller.

$$T_{rr,rl} = \frac{1}{2}T_{driver} \tag{36}$$

$$T_{fr,fl} = \pm\Delta T \tag{37}$$

Front Wheel Drive + Rear Torque Vectoring:

An inverse of the above stated controller.

$$T_{fr,fl} = \frac{1}{2}T_{driver} \tag{38}$$

$$T_{rr,rl} = \pm\Delta T \tag{39}$$

C. Proposed Control Method

Fig. 5 shows the block diagram of the controller and vehicle model.

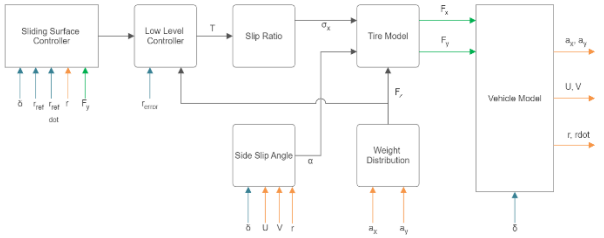

Fig. 5 Control Structure Block Diagram

The following method involves the use of a combination of the above stated controllers and the distribution of torques according to the ratio of normal forces on each tire.

The main control strategy comprises of three 'modes' or different distribution dependant on a set of user defined thresholds. These thresholds can be used to alter and tune the response and overall performance characteristics of the vehicle.

Mode 1:

The rear axle is driven and the front axle is used for torque vectoring. This configuration is chosen for relatively easy manoeuvres. The fact that the IWMs can only produce a limited amount of torque means that each axle has to handle one input i.e. T_{driver} and ΔT reducing the chances of reaching saturation.

$$T_{rr,rl} = \frac{1}{2}T_{driver} \tag{40}$$

$$T_{fr,fl} = \pm\Delta T \tag{41}$$

where ΔT is:

$$\Delta T = \frac{M_z R_{eff}}{halftrack} \tag{42}$$

Mode 2:

When the yaw rate tracking error is above a specified threshold, both axles are now provided with corrective torques according to the ratio of the normal forces on each tire. This enables both axles to now contribute to generating the corrective yaw moment.

$$T_{rr} = \frac{1}{2}T_{driver} + Tv_{rr} \tag{43}$$

$$T_{rl} = \frac{1}{2}T_{driver} - Tv_{rl} \tag{44}$$

$$T_{fr} = +Tv_{fr} \tag{45}$$

$$T_{fl} = -Tv_{fl} \tag{46}$$

The torque vectoring forces for each tire being:

$$Tv_{fr} = Tv_{total}\left(\frac{zfr}{zfr+zrr}\right) \tag{47}$$

$$Tv_{fl} = Tv_{total}\left(\frac{zfl}{zfl+zrl}\right) \tag{48}$$

$$Tv_{rr} = Tv_{total}\left(\frac{zrr}{zfr+zrr}\right) \tag{49}$$

$$Tv_{rl} = Tv_{total}\left(\frac{zrl}{zfl+zrl}\right) \tag{50}$$

where Tv_{total} is:

$$Tv_{total} = \frac{M_z R_{eff}}{halftrack} \tag{51}$$

Mode 3:

When the yaw rate tracking error is above the second specified threshold, the base or the driver torque is also divided across the rear axle according to the ratio of the normal forces on each tire. Authors in [14] show that the cornering potential improves when the driving force is also distributed. This however, causes the overall longitudinal speed to drop more than before but as the speed decreases it results in improved yaw rate tracking. The threshold can be set in order to activate this mode in extreme driving conditions such as low friction roads.

$$T_{rr} = \frac{1}{2}T_{driver} + (0.5 * Tv_{total}) \tag{52}$$

$$T_{rl} = \frac{1}{2}T_{driver} - (0.5 * Tv_{total}) \tag{53}$$

$$T_{fr} = +(0.5 * Tv_{total}) \tag{54}$$

$$T_{fl} = -(0.5 * Tv_{total}) \tag{55}$$

These are then distributed according to ratio of the normal forces on each tire:

$$Tv_{fr} = T_{rr}\left(\frac{zfr}{zfr+zrr}\right) \tag{56}$$

$$Tv_{fl} = T_{fl}\left(\frac{zfl}{zfl+zrl}\right) \tag{57}$$

$$Tv_{rr} = T_{rr}\left(\frac{zrr}{zfr+zrr}\right) \tag{58}$$

$$Tv_{rl} = T_{rl}\left(\frac{zrl}{zfl+zrl}\right) \tag{59}$$

where Tv_{total} is:

$$Tv_{total} = \frac{M_z R_{eff}}{halftrack} \tag{60}$$

Note: The thresholds of yaw rate error for the 'Experimental' controller are set as follows:

- Mode 2: 0.01
- Mode 3: 0.05

V. RESULTS

The main input signals to the high level controller (HLC) are the steering angle, the yaw rate of the vehicle and the desired yaw rate whereas the low level controllers (LLC) receive the requested drive torques from the driver and the desired corrective moment from the HLC.

The simulations were carried out for multiple lane change manoeuvres, at first the coefficient of friction is 1 and then after 10s, coefficient of friction changes to 0.5 in order to replicate a damp or slippery patch on the road.

A simple P (proportional) controller was used for cruise control at a set longitudinal velocity of 20m/s. The torque input for each wheel is capped to 400 Nm as the electric motors are unable to produce very high amounts of torque in practical applications.

A sine steering input as shown below in Fig. 6 is used as shown below with an amplitude of 6 degrees (1.05 rad) which corresponds to 90 degrees of steering wheel rotation if steering ratio of 15:1 is considered.

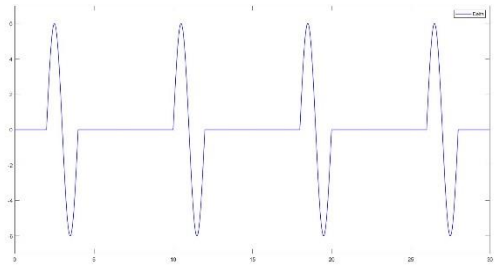

Fig. 6 Sine Steering Input

A. Dry Road Conditions

The simulation is carried out for 30 seconds in which 4 complete sweeps of the sine signal are achieved.

Following figures show the results for the first complete sweep.

Yaw Rate:

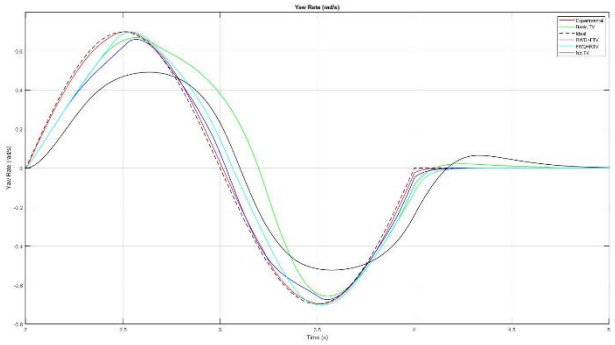

Fig. 7 Yaw Rate (rad/s) vs. Time (s) (Red-Proposed Controller, Green-Basic, Dashed-Ideal, Blue-RWD+FTV, Cyan-FWD+RTV, Solid Black-No TV)

Yaw Rate Error:

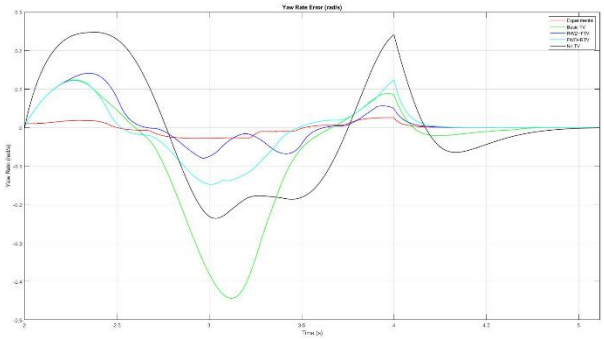

Fig. 8 Yaw Rate Error (rad/s) vs. Time (s) (Red-Proposed Controller, Green-Basic, Dashed-Ideal, Blue-RWD+FTV, Cyan-FWD+RTV, Solid Black-No TV)

Vehicle Speed:

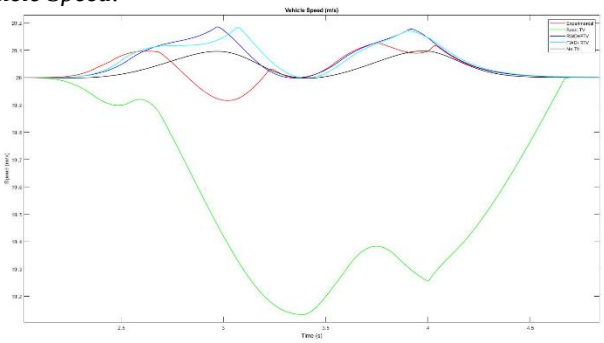

Fig. 9 Vehicle Speed (m/s) vs. Time (s) (Red-Proposed Controller, Green-Basic, Dashed-Ideal, Blue-RWD+FTV, Cyan-FWD+RTV, Solid Black-No TV)

All controllers apart from the 'Basic' controller are able to relatively maintain the set speed by the driver.

Vehicle Position:

Fig. 10 below shows the tracking performance of the vehicle.

Note: This figure is a result of full 30 seconds of simulations.

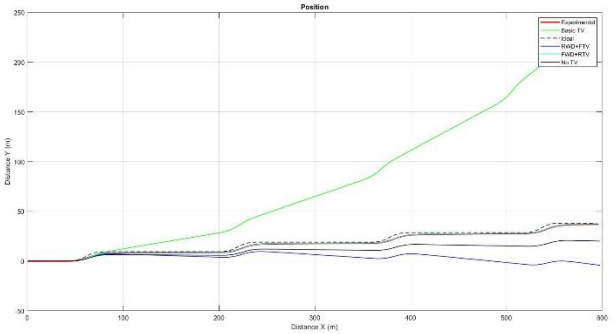

Fig. 10 Vehicle Position Comparison (Red-Proposed Controller, Green-Basic, Dashed-Ideal, Blue-RWD+FTV, Cyan-FWD+RTV, Solid Black-No TV)

As seen here the proposed and 'FWD+RTV' controllers both follow the ideal path with least deviation.

B. Slippery Road Conditions

Following figures show the results for the first complete sweep under slippery conditions.

Yaw Rate:

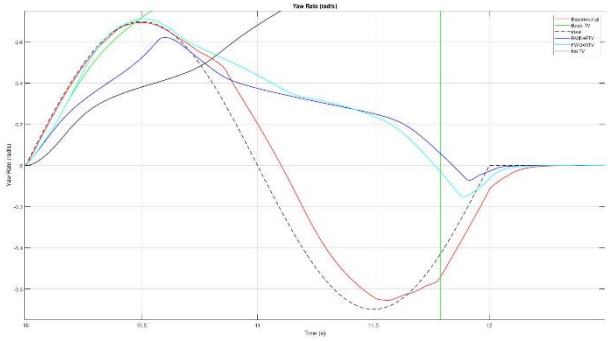

Fig. 11 Yaw Rate (rad/s) vs. Time (s) (Red-Proposed Controller, Green-Basic, Dashed-Ideal, Blue-RWD+FTV, Cyan-FWD+RTV, Solid Black-No TV)

The vehicle without torque vectoring and the 'Basic' controller both are unable to cope as the high yaw rate values indicate that the vehicle has spun out of control. 'RWD+FTV' and the 'FWD+RTV' controllers are able to keep the vehicle from losing control and return to a state of no change in the yaw motion of the vehicle.

Yaw Rate Error:

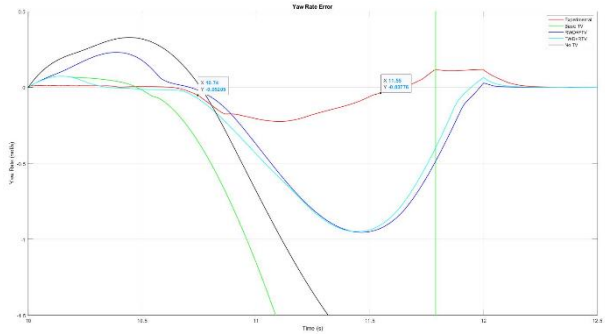

Fig. 12 Yaw Rate Error (rad/s) vs. Time (s) (Red-Proposed Controller, Green-Basic, Dashed-Ideal, Blue-RWD+FTV, Cyan-FWD+RTV, Solid Black-No TV)

As seen above, the proposed controller and the other controllers are able to eventually reach zero error unlike the basic TV controller and the vehicle with no TV.

Vehicle Speed:

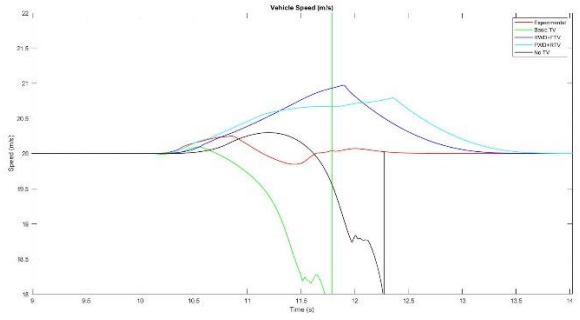

Fig. 13 Vehicle Speed (m/s) (Red-Proposed Controller, Green-Basic, Dashed-Ideal, Blue-RWD+FTV, Cyan-FWD+RTV, Solid Black-No TV)

Vehicle Position:

Fig. 14 below shows the tracking performance of the vehicle.

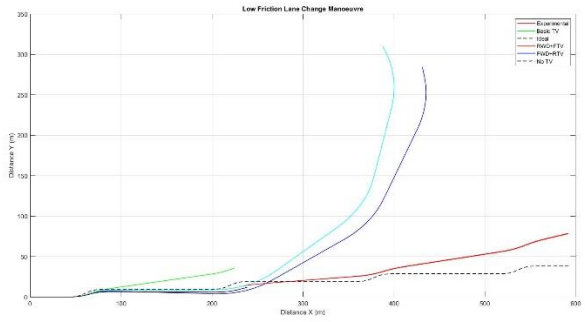

Fig. 14 Vehicle Position (Red-Proposed Controller, Green-Basic, Dashed-Ideal, Blue-RWD+FTV, Cyan-FWD+RTV, Solid Black-No TV)

Here again, the 'Base' controller and the vehicle with no TV are not able to register their position.

VI. DISCUSSION

The results show a significant improvement in yaw rate tracking in the vehicle with the proposed control strategy. For the first manoeuvre, the yaw rate error for this controller is the lowest at its peak, a deviation of 0.0258 rad/s compared to 0.0561 rad/s of the next best controller. The proposed control strategy also outperforms other controllers in slippery conditions with the maximum deviation of 0.117 rad/s compared to the next best controller's value of 0.95 rad/s.

For slippery road conditions, the conventional controllers struggle to track the desired yaw rate for most of the manoeuvre. The proposed controller on the other hand outperforms them and is able to track the required yaw rate more closely in low grip conditions.

The region between 10.7s and 11.5s shows significant improvement in tracking when compared to other controllers. This is where mode 3 is active as shown in Fig. 15.

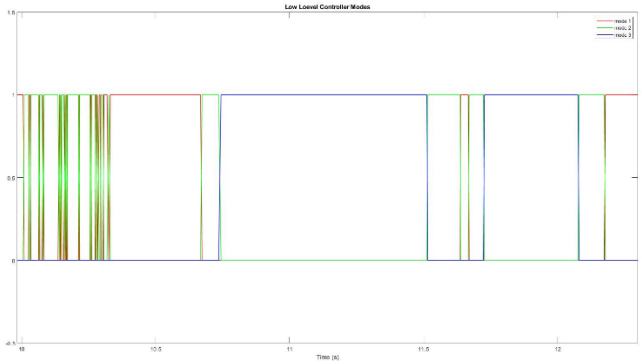

Fig. 15 Modes in the Proposed Controller (Red-Mode 1, Green-Mode 2, Blue-Mode 3)

When comparing the change in speed, the proposed strategy proves to be the most stable with least deviation from the set speed of 20 m/s in both scenarios. The decrease in vehicle speed for the proposed controller in the first scenario is marginal compared to the performance decline caused by the 'Basic TV' controller. This is because the torques required by the 'Basic TV' controller are much higher than the available 400Nm at the rear IWMs and results in saturation as shown in Fig. 16 below.

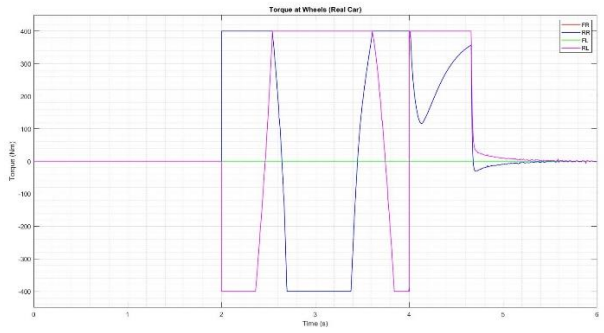

Fig. 16 Torque (Nm) at Individual Wheels for the Basic Controller (Red-FR, Blue-RR, Green-FL, Magenta-RL)

Even though a decrease in vehicle speed is expected during the application of mode 3 as the driving torques are also distributed, the decrease in vehicle speed for the 'Experimental' controller is very low and it is easier for the speed controller to stick to the constant speed specified by the user. Whereas the 'FWD+RTV' and the 'RWD+FTV' controllers both increased the vehicle speed above the set value which can be a safety hazard.

Comparing the vehicle position graphs, it is clear that the proposed controller shows the best tracking followed by the 'RWD+FTV' controller in slippery conditions.

VII. CONCLUSION

The aim of this work was to improve the stability and performance of the vehicle in different conditions through the use of a novel torque vectoring strategy. Simulations and their results indicate that the proposed controller is indeed able to improve the overall stability and tracking performance of the vehicle. Furthermore, the proposed strategy is not only able to keep the vehicle from spinning in extreme conditions where other controllers fail but outperforms them. The application of the third mode during low grip conditions enables the vehicle to closely follow the set speed and not exceed it by a large value which can be a cause for safety concern.

However, further improvements to this study could include the use of Magic Formula tire model to understand tire usage and limits in a more realistic manner.

REFERENCES

[1] C. Poussot-Vassala, O. Senameb, L. Dugardb and S.M. Savaresi, "Vehicle Dynamic Stability Improvements Through Gain-Scheduled Steering and Braking Control," in *Vehicle System Dynamics Vol. 00, No. 00, January 2009, 1–28*.

[2] Jalali, Kiumars & Uchida, Thomas & Lambert, Steve & McPhee, John., "Development of an Advanced Torque Vectoring Control System for an Electric Vehicle with In-Wheel Motors using Soft Computing Techniques," *SAE International Journal of Alternative Powertrains. 2. 261-278. 10.4271/2013-01-0698* (2013).

[3] V. Scheuch, G. Kaiser, M. Korte, P. Grabs, F. Kreft and F. Holzmann "A safe Torque Vectoring function for an electric vehicle," in *2013 World Electric Vehicle Symposium and Exhibition (EVS27)*, 2013, pp. 1-10.

[4] Yang, Derong & Idegren, Martin & Jonasson, Mats., "Torque Vectoring Control for Progressive Cornering Performance in AWD Electric Vehicles," in *Proc. AVEC '18*, 2018.

[5] S. M. Metev and V. P. Veiko, *Laser Assisted Microtechnology*, 2nd ed., vol 73, Springer, Cham, 2019.

[6] Norhazimi Hamzah; M Khairi Aripin; Yahaya Md Sam; Hazlina Selamat; Muhamad Fahezal Ismail, "Vehicle stability enhancement based on second order sliding mode control," *2012 IEEE International Conference on Control System, Computing and Engineering*

[7] E. Esmailzadeh, A. Goodarzi, G.R. Vossoughi, "Optimal yaw moment control law for improved vehicle handling" *Mechatronics, 13(7), 659-675.*, (2003)

[8] IşılayYoğurtçuS. S. Solmaz, Selahattin Caglar Baslamisli, "Lateral stability control based on active motor torque control for electric and hybrid vehicles." *In 2015 IEEE European modelling symposium (EMS) (pp. 213-218). IEEE.*, (2015)

[9] J. Antunes, A. Antunes, P. Outeiro, C. Cardeira and P. Oliveira, "Testing of a torque vectoring controller for a Formula Student prototype," *Robotics and Autonomous Systems, 113, 56-62,* (2019)

[10] R. Rajamani., "Vehicle dynamics and control, Springer Science & Business Media., (2011)

[11] Stoop, A.W., "Design and implementation of torque vectoring for the forze racing car," Doctoral dissertation, Delft University of Technology, 2014

[12] Daniel Rubin; Shai Arogeti, "Vehicle Yaw Stability Control Using Rear Active Differential via Sliding Mode Control Methods," in *2013 21st Mediterranean Conference on Control and Automation, MED 2013 - Conference Proceedings. 10.1109/MED.2013.6608740.*

[13] J. Ghosh, A. Tonoli and N. Amati, "A Torque Vectoring Strategy for Improving the Performance of a Rear Wheel Drive Electric Vehicle," *2015 IEEE Vehicle Power and Propulsion Conference, VPPC 2015,* (2015, December 10)

[14] K. Sawase, Yuichi Ushiroda, "Improvement of Vehicle Dynamics by Right-and-Left Torque Vectoring System in Various Drivetrains x," mitsubishi motors technical review 2008 No.20

[15] Mangia, A., Lenzo, B. & Sabbioni, E., "An integrated torque-vectoring control framework for electric vehicles featuring multiple handling and energy-efficiency modes selectable by the driver, Meccanica 56, 991–1010 (2021)

[16] H.E. Tseng; B. Ashrafi; D. Madau; T. Allen Brown, D. Recker, "The development of vehicle stability control at Ford," *IEEE/ASME Transactions on Mechatronics (Volume: 4, Issue: 3, September 1999)*

[17] J. Ghosh, A. Tonoli and N. Amati, "Improvement of Lap-time of a Rear Wheel Drive Electric Racing Vehicle by a Novel Motor Torque Control Strategy," in *SAE Technical Paper 2017-01-0509, 2017.*